Received January 10, 2022, accepted February 9, 2022, date of publication February 16, 2022, date of current version March 1, 2022.

Digital Object Identifier 10.1109/ACCESS.2022.3152205

A Novel Switching Methodology for Low Voltage Static Regulators

RODRIGO NOBIS DA COSTA LIMA AND JOSÉ RUBENS MACEDO, JR., (Senior Member, IEEE)
Faculty of Electrical Engineering, Federal University of Uberlandia, Uberlandia 38408-014, Brazil

Corresponding author: Rodrigo Nobis da Costa Lima (rodrigonobis@hotmail.com)

This work was supported by the Brazilian National Council for Scientific and Technological Development (CNPq) under Grant 140651/2018-7.

ABSTRACT This paper presents a new switching methodology for low voltage static regulators. The switching method proposed in this paper differs from those found in the literature due to it not needing a measurement of the current signal in the transformer tap windings and/or in the static switches. This method simplifies the control, reduces the cost of implementation, and allows safe application onto grids with low loading and high harmonic current distortion. In order to analyze and evaluate the performance of the proposed methodology, the static voltage regulator presented in this article was implemented in a computer simulation and, later, a laboratory prototype was built. The topology, the operational principles, and the specifications of its constituent components are discussed and presented in this paper. In addition, the prototype of the equipment was tested under three different load conditions: operating under no-load conditions, supplying a purely resistive load and supplying a nonlinear load. For each of the three types of loads considered, the static voltage regulator's performance was evaluated using specific measurements, which considered the occurrence of both long and short duration voltage variations imposed on the input of the equipment by a programmable power source. The obtained results show that—in the worst-case scenario—the tap changing process takes less than 4 cycles of the fundamental frequency to be concluded. In light of the obtained performance, the proposed switching methodology for low voltage static regulators is a promising solution for large scale use under varied applications.

INDEX TERMS Static voltage regulator, on-load tap changing, long duration voltage variations, short duration voltage variations, power quality.

I. INTRODUCTION

Long and short duration voltage variations are the disturbances most commonly related to power quality on electric systems. Maintaining steady-state voltage amplitude within an acceptable range is the elementary requirement for good operability of nearly all loads connected to electric systems. However, those loads based on switched power supplies (wide range of tolerable input voltage) present greater tolerance to long duration voltage variations. Nevertheless, at the same time, they are relatively sensitive to short-duration voltage variations. Another important aspect of voltage regulation in distribution grids is the increase of distributed generation, especially photovoltaic generation, which has an intermittent characteristic. The mechanical on-load tap changers, one of the most employed equipment to regulate voltage in distribution systems, do not have a sufficiently short response time to attenuate the momentary voltage variations caused by photovoltaic systems [1]. In this context, static voltage regulators (SVRs) have been highlighted among the possible solutions for voltage control on electric grids. This is because SVRs can regulate the steady state voltage, like conventional electromechanical regulators, and attenuate short duration voltage variations, once they can switch their taps in a matter of few fundamental frequency cycles.

When it comes to long duration voltage variations, the standard ANSI C84.1 [2], for example, defines the rated system voltages to be adopted on electric grids and presents the acceptable voltage range for electric energy systems operating at 60 Hz in the USA. In the case of three-phase systems 208Y/120V, the acceptable range for the operational voltage sits between 106V and 127V for phase-to-neutral voltages, and between 184V and 220V for phase-to-phase voltages. In the case of short duration voltage variations, there also exist

The associate editor coordinating the review of this manuscript and approving it for publication was Jahangir Hossain.

innumerous standards. However, as a rule, these standards—as in the example of IEEE 1159-2019 [3]—classify the short duration voltage variations as being voltage events with amplitudes lower than 90% (voltage sags) or higher than 110% (voltage swells) of the RMS voltage. In both cases, the duration of events should be of a 1/2 cycle to 1 minute. Voltage events with a duration higher than 1 minute are classified as long duration voltage variations.

Currently, as one of the diverse solutions to make the supply voltage compatible with the operating range of loads and comply with existing regulations on the subject, different technologies for static voltage regulators have been studied and presented in the technical literature and the market. Theoretically, SVRs promote static switching between different windings on a magnetic array, altering the output voltage in relation to the input voltage without moving parts, as is the case of electromechanical regulators.

One of the first studies related to the conception of an SVR dates back to 1970 [4]. In this pioneering study, the author proposes an autotransformer that has its output voltage regulated by TRIACs. The voltage regulation is achieved by varying the firing angle of the switches that activate the secondary winding. As the control varies the voltage width of a fixed winding, this method requires fewer taps. However, its operation can cause expressive voltage harmonic distortions to the load, depending on the firing angle of the static switches. Reference [5] presents a similar static voltage regulation methodology by varying the firing angles of thyristors, which is differentiated from [4] by the proposed magnetic apparatus and the utilized static switches.

Since then, several methodologies that employ power electronics in voltage regulation have been presented. Initially, static switches were used as auxiliary components of the tap switching circuit in conventional electromechanical regulators to constitute the denominated hybrid voltage regulators. Nevertheless, the use of static switches as an auxiliary component had the underlying objective to attenuate the electric arcs resulting from the tap changing process without impacting the voltage regulation speed.

References [6] and [7] present application examples of hybrid regulators. In these two papers, the authors propose an auxiliary switching circuit composed of thyristors, which, during the tap change, has the objective of providing a path to the portion of the switching circuit current that would be mechanically interrupted. The mechanical interruption of the current results in an electrical arc capable of damaging the contacts of the mechanical switches and degrading the insulating oil over the lifespan of the equipment. Therefore, at first, the purpose of static switches was to preserve the mechanical contacts of the regulator switching apparatus, attenuating or even eliminating the presence of electrical arcs during tap changing.

Even over recent years, new methodologies for switching in hybrid regulators have been published in the literature, as shown in [8]–[10].

The authors in [8] propose a new conception of a switching circuit comprising mechanical and static switches. The equipment presented in this paper employs two sets of static switches to perform the tap changing: the first set of switches must be capable of interrupting currents, such as IGBTs and IGCTs, for example. Meanwhile, the second set does not need to have this functionality, and both thyristors and IGBTs can be used, for example. In this study, the static switches alter the taps, and the mechanical switches conduct the current only in steady state. However, the static tap change associated with this methodology depends on the knowledge of the polarity and, as a consequence the measurement, of the voltage and current signals of the taps. As will be discussed below, this can be a limiting factor for applying the methodology under certain operational conditions, such as in situations with low loading and high levels of harmonic distortion.

In [9], the authors propose a hybrid voltage regulator composed of vacuum switches, responsible for the mechanical activation of the tap windings and thyristors, allocated into an auxiliary circuit tasked with dissipating the switching energy, which would be dissipated in the form of an electric arc. Nonetheless, the tap changing of the regulator presented in this paper must be done when the current crosses zero. Similar to the methodology described in [8], the tap change methodology proposed in [9] is dependent on the adequate measurement of the current waveform of the taps, which can be a problem under some operational situations, as previously cited.

Reference [10], on the other hand, presents an auxiliary electronic apparatus capable of zeroing the current on one of the two switching reactor windings of an electromechanical regulator. As such, performing the change from one tap to another in mechanical form does not interrupt any current in the switching circuit, thus mitigating, or even extinguishing, the presence of electrical arcs during the tap change. This methodology does not require the knowledge of the zero crossing of the tap current to perform the switching, thus proving to be a safer hybrid regulator switching method than its predecessors.

However, the evolution of static switches technology placed power electronics at the forefront of a new type of equipment—the fully static voltage regulator. In this new scenario, different static switching methodologies were added to the technical literature over the years [11]–[14].

The study in [11] presents a computational simulation of a Dynamic Voltage Regulator (DVR) based on the static tap change of a transformer. In the fully static proposed DVR, the voltage applied to the series transformer is controlled by thyristors switching taps of an auxiliary transformer. The concerning point of the methodology presented in this paper is the need to know the instant of the zero-crossing of the switches' voltages and current signals. If the triggering of the switches is performed off the current zero-crossing instant, the auxiliary transformer would be short-circuited or even a dangerous overvoltage can occur on the primary

side of the series transformer due to the overexcitation of its magnetic core.

Reference [12] proposes a two-winding transformer with static regulation, using thyristors, performed through electronic activation of the taps on its primary. In this methodology, the control must trigger the thyristors at specific moments of the voltage and current waveforms, determined by the phase displacement of these two signals. Similar to the previously referenced document, this switching methodology is highly dependent on the knowledge and correct measurement of the switches' current and its zero-crossing moment. Depending on the operating situation of the electrical grid where the equipment is installed, this requirement can be difficult to achieve.

The study in [13] also presents a transformer of two windings with full static regulation performed on its primary. The authors propose using TRIACs as static switches, since these are bidirectional devices, thus decreasing the number of electronic switches in the equipment. In this paper, the control sends commands for the opening and closing of the TRIACs at the zero-crossing moment of its currents, and the measurement and precise identification of this instant of the waveform are decisive in the adequate operation of the proposed regulator.

In [14], the authors also present a two-winding transformer with static regulation performed by switching the primary taps. However, in contrast to studies [12] and [13], the authors propose using IGBTs as static switches. This guarantees greater flexibility and safety during tap changes since these switches can interrupt their current at moments other than their zero-crossing, at the cost of a overvoltage on their terminals. However, the IGBTs are triggered at the instant of their current zero-crossing to minimize the overvoltage and guarantee the operational safety of the switches. Once again, the tap change control in the proposed methodology depends on the knowledge of the zero-crossing instant of the switches' current, which can be a restricting factor in the application of this switching method.

In reference [15], the authors propose several steps to ensure an optimal specification of an SVR. These steps mention the number of tap windings and voltage ratings, ratings of the static switches, the presentation of the control, and its variables and diagrams. The authors also present a low power SVR prototype employing the optimal methodology described along the document. The developed prototype employs a two-winding transformer with its secondary divided into taps as its magnetic apparatus. As in [14], the static switches used in the prototype are IGBTs. The tap change is completed in approximately five cycles. However, similar to the previously referenced control methodologies, the triggering of the switches is performed when the current crosses zero, so that the proper current signal measurement is vital for the control and safety of the equipment.

Reference [16] also proposes an SVR that employs IGBTs as static switches. In this paper, the switches are installed on the primary side of a two-winding transformer and, similar to the switching methodologies presented above, the control only triggers the IGBTs when their current crosses zero. In order to guarantee the safe application of this switching methodology, it is essential to measure the current waveform correctly, which can be a limiting factor for its application in low load situations and/or in grids that present high current harmonic distortion.

The authors in [17] present a methodology that does not need the identification of the current zero-crossing instant and uses only the polarity information of the current circulating through a tap. This tap changing method is less complex than previous ones. Nevertheless, it can also lead to equipment misoperation in situations with low amplitude currents and high levels of harmonic distortion.

Given the above, it can be concluded that the switching methodologies found in the technical literature are dependent on current measurements of the switches and/or of the windings and on the knowledge of its zero-crossing instant. This increases the number of current sensors and control complexity, mainly in equipment with a high number of switches. In addition, the zero-crossing point of the current may not be defined clearly in situations of low load and high current harmonic distortion.

In light of the above mentioned, the study here presents a new switching methodology for static voltage regulators, presenting as a pronounced differential the fact that it does not require the measurement of switches or winding currents. Another differential of the proposed methodology in relation to most of those referenced above is the use of TRIACs as static switches, which reduce by half the quantity of switches and, consequently, the number of triggering circuits needed.

Table 1 summarizes the comparison between the methodology proposed in this article and the aforementioned works referenced, indicating the type of regulator (hybrid or fully static), the need to measure the current signal by the control, the static switches used, and to determine whether the equipment is responsible for distorting the waveform of its output voltage.

To validate the effectiveness of the proposed methodology, the new static switching methodology will be presented, and constructive characteristics of the prototype will be developed in the following sections. The results denoting the computational simulation of the SVR, implemented with the constructive characteristics and electrical parameters raised in the third section, will be presented in the sequence. Finally, the last section of this paper presents the results of laboratory tests performed on the developed prototype, which demonstrate that the new proposed methodology is very promising to attenuate long and short duration voltage variations.

II. A NEW SWITCHING METHODOLOGY FOR STATIC VOLTAGE REGULATORS

The schematic of the power circuit of the proposed static voltage regulator is shown in Fig. 1. The equipment is composed of an autotransformer, with its secondary winding divided into two distinct taps. The TRIACs S_1 to S_8 perform the

TABLE 1. Comparison between the referenced methodologies and the new proposed switching methodology.

References	Type	Switches' current measurement	Employed static switches	Voltage harmonic distortion
[4-5]	Fully static	No	Thyristors	Yes
[6-7]	Hybrid	No	Thyristors	No
[8]	Hybrid	Yes	IGBTs with Thyristors or IGBTs	No
[9]	Hybrid	Yes	Thyristors	No
[10]	Hybrid	No	Not informed	No
[11-12]	Fully static	Yes	Thyristors	No
[13]	Fully static	Yes	TRIACs	No
[14-17]	Fully static	Yes	IGBTs	No
Proposed novel methodology	Fully static	No	TRIACs	No

TABLE 2. Switches triggered in each tap position.

Tap position	Switches triggered
0	S_3 and S_4
Intermediate +1	S_2 and S_3
+1	S_2, S_3 and S_7
Intermediate +2	S_4 and S_5
+2	S_4, S_5 and S_8
Intermediate +3	S_2 and S_5
+3	S_2, S_5, S_7 and S_8
Intermediate –1	S_1 and S_4
–1	S_1, S_4 and S_7
Intermediate –2	S_3 and S_6
–2	S_3, S_6 and S_8
Intermediate –3	S_1 and S_6
–3	S_1, S_6, S_7 and S_8

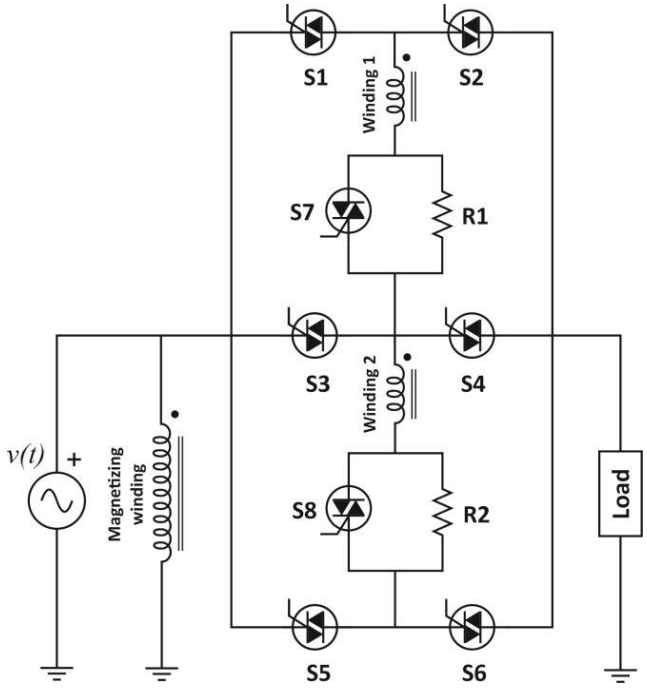

FIGURE 1. Schematic of the developed SVR.

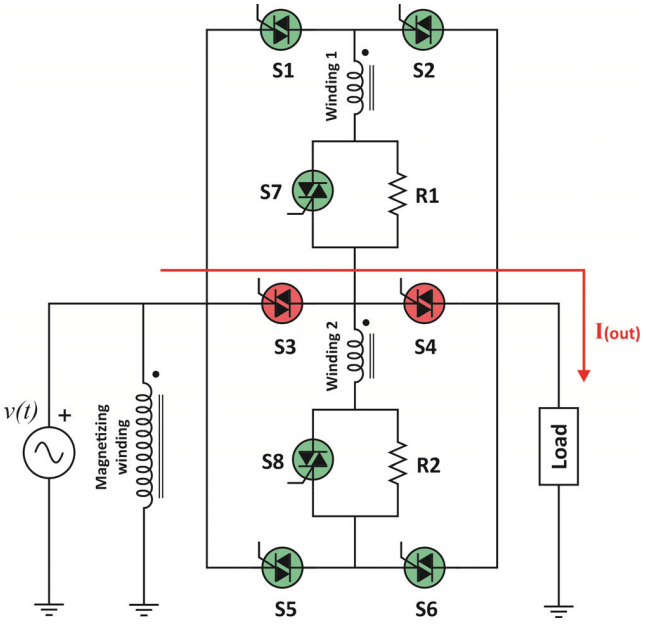

FIGURE 2. SVR in the position of tap 0.

switching, and the resistors R_1 and R_2 limit an eventual short-circuit current during the tap changing process.

The presence of the switching resistors allows the tap changing to occur without the need to monitor the switches and/or tap currents. The change from one tap to another requires the passing through an intermediary tap, where the switching resistors are put into operation, thus limiting an eventual short-circuit of the tap windings, as mentioned previously. Table 2 shows the switches from Fig. 1 that will be triggered in each of the possible tap positions of the proposed equipment.

For example, the change of the tap from position 0 to position +1 needs the SVR to trigger the intermediary tap +1 before the activation of tap +1. For illustration purposes, the three stages of this tap changing are presented in Figs. 2, 3, and 4, respectively.

The switching from tap 0 to intermediate tap +1 requires triggering on switch S_4 and triggering off S_2. However, if the current circulating through switch S_4 is not crossing zero at the instant switch S_2 is triggered on, there may occur a short-circuit of winding 1, indicated by I_{sc} in Fig. 3. Nevertheless, the reasonably elevated current will be controlled by switching resistance R_1. Therefore, the short-circuit will remain until the current of switch S_4, composed

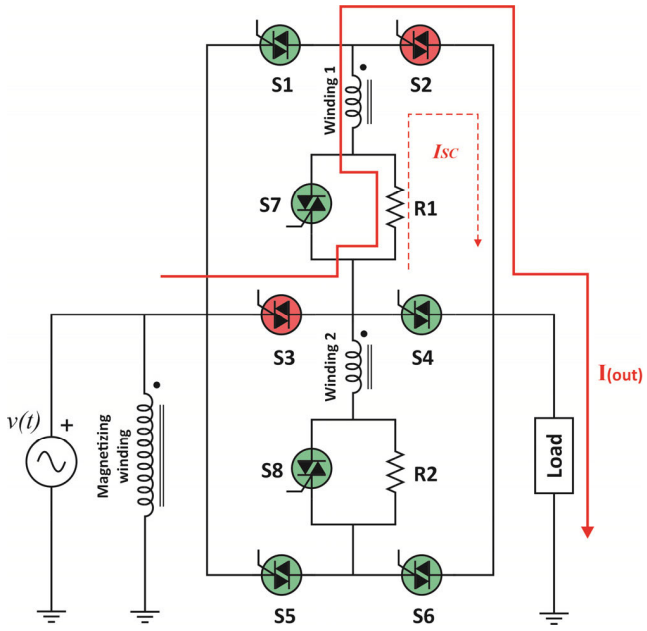

FIGURE 3. SVR in the position of intermediary tap + 1.

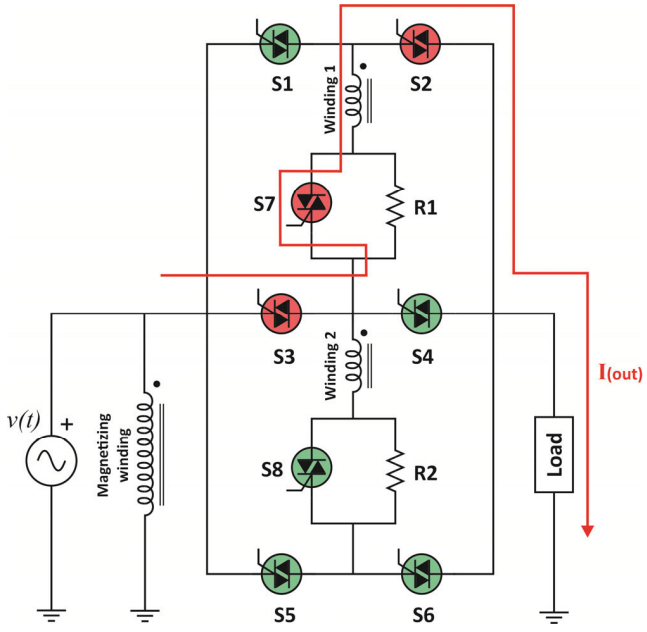

FIGURE 4. SVR in the position of tap +1.

of the load current added to the short-circuit current, crosses zero after the removal of the S_4 gate signal.

To guarantee that the current of switch S_4 passes through zero and this switch opens, the control waits for 3/4 cycle of the fundamental frequency before triggering switch S_7, thus finalizing the tap changing process from position 0 to position +1, as presented in Fig. 4.

The amplitude of the RMS output voltage of the SVR is calculated using windows of one cycle with half-cycle sliding, employing a sampling rate of 3840 Hz (64 samples/cycle of 60 Hz). This way, the equipment can delay 0.5 to 1.5 cycles to detect voltage variations depending on the start time of each variation in relation to the instantaneous voltage waveform and the amplitude of the variation. The more the event distances itself from the acceptable voltage level (in terms of amplitude), the quicker the SVR control system detects it. In order to obtain a more accurate RMS output voltage of the event, the control waits for 1/2 cycle before determining the tap position and triggering the switches. This is due to the half-cycle sliding window of the RMS calculation, in a way that the first RMS voltage of the event may be considering voltage samples from before the start of the event. This results in an intermediary value between voltage values measured before and during the voltage variation.

In the same way, after triggering the switches of the intermediate tap, the SVR control waits for 3/4 of a cycle before triggering the final tap switches. This intentional delay guarantees that the current of the switches receiving the command to open passes through zero, securing their effective opening.

The tap switching process lasts less than 4 cycles to be completed, as will be shown in Sections IV and V, which presents the simulations and tests results of the proposed static voltage regulator prototype, respectively.

Highlighted here is that the change of taps from positive to negative positions, and vice-versa, requires that the SVR always passes through the tap 0 before reversing the voltage compensation polarity. The flowchart of the switching algorithm for the new SVR developed herein is presented in Fig.5.

III. CONSTRUTIVE CHARACTERISTICS OF THE STATIC VOLTAGE REGULATOR PROTOTYPE EMBEDDED WITH THE PROPOSED NEW SWITCHING METHODOLOGY

A laboratory prototype static voltage regulator was developed to present the effectiveness of the switching methodology described in the previous section. The main components of the developed equipment are presented in the following.

A. AUTOTRANSFORMER

The basic parameters of the autotransformer used in the SVR prototype are listed in Table 3.

The rated voltage of the entire tap winding (winding 1 + winding 2), equal to 50.8 Volt (0.4 pu), was chosen to limit the output voltage of the SVR at 1.4 pu when its input voltage values 1.0 pu. This situation can occur when the equipment is correcting a voltage sag that requests the triggering of tap +3 and the input voltage returns to its rated value. As the tap changes take less than 4 cycles to be finalized, the load is expected to be subjected to 1.4 pu of voltage during this short period. Recent thermal and dielectric withstand tests performed on domestic appliances showed voltage withstand limits much higher than the aforementioned operating conditions. In [18], for example, tests were performed on television sets, stereo equipment, and computers. Among the tested equipment, the one with the lowest withstand was damaged only with voltages higher than 2.0 pu after 46 cycles. Similarly, the study presented in [19] performed withstand tests on different domestic appliances, such as refrigerators,

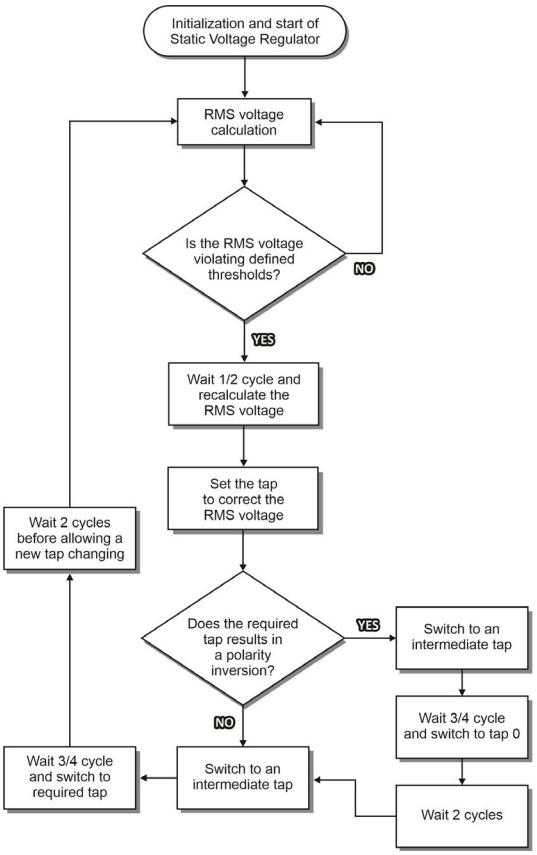

FIGURE 5. Flowchart of the SVR switching algorithm.

TABLE 3. Autotransformer rating.

Quantity	Value
Rated power	1.5 kVA
Magnetizing winding rated voltage	127 V
Magnetizing winding impedance	0.4051 + j0.5321 %
Winding 1 rated voltage	19.05 V (0.15 pu)
Winding 1 impedance	0.1519 + j0.1995 %
Winding 2 Rated Voltage	31.75 V (0.25 pu)
Winding 2 impedance	0.2532 + j0.3325 %
Winding 1 + winding 2 Rated Voltage	50.8 V (0.4 pu)
Core shunt resistance	75.669 %
Core shunt inductive reactance	24.225 %
Rated frequency	60 Hz
Number of phases	1

freezers, washing machines, and air conditioning units. The results showed that the equipment with the lowest withstand (washing machine) was damaged only when subjected to a voltage with an amplitude of 1.4 pu for 10 seconds.

In light of the above, no failures or damage to electrical equipment are expected when submitted to voltages of amplitudes up to 1.4 pu for less than 4 cycles. Even so, if it is desired to increase the operational safety margin of the SVR, the rated voltage of the taps can be reduced at the cost of decreased regulation range.

B. SWITCHING RESISTORS

The switching resistors R_1 and R_2, indicated in Fig.1, define the limit of the current in eventual short-circuits on the windings, which can occur during the tap changing process. These resistors were designed to limit the short-circuit current in the windings to values of no higher than 3.0 pu of the autotransformer rated current when the input voltage is equal to 1.4 pu, in accordance with (1) to (4):

$$R_1 = \frac{V_{in} \times V_{tap1}}{I_{sc}} = \frac{1.4 \times 0.15}{3} = 0.070\ pu \quad (1)$$

$$R_1 = 0.753\ \Omega \quad (2)$$

$$R_2 = \frac{V_{in} \times V_{tap2}}{I_{sc}} = \frac{1.4 \times 0.25}{3} = 0.117\ pu \quad (3)$$

$$R_2 = 1.258\ \Omega \quad (4)$$

where R_1 is the resistance value of resistor R_1, V_{in} is the RMS input voltage of the SVR in pu, V_{tap1} is the tap 1 rated RMS voltage in pu, R_2 is the resistance value of resistor R_2, V_{tap2} is the tap 2 rated RMS voltage in pu.

It can be observed that the percentual impedance of the autotransformer, as well as the grid short-circuit impedance, were not taken into consideration in the previous equations, thus leading to more conservative resistor values. In real applications, wherein the grid and autotransformer impedances have non-zero values, magnitudes of less than 3.0 pu are expected for winding short-circuit currents. Furthermore, 1.4 pu swells are not frequent events in real systems. This implies that the calculation of switching resistors presented above is extremely conservative, to ensure safe operation for static switches and tap windings.

Nevertheless, as aforementioned, the short-circuit current in the windings will be present as long as the currents of the switches that had their gate signal removed do not pass through zero. Ideally, this period has a maximum duration of 1/2 cycle. In any case, to reach higher operational safety, the SVR control waits for 3/4 of a cycle before carrying out the tap changing procedure. The power dissipation capacity of the resistors in the equipment prototype was specified to withstand the rated autotransformer current, even though they are operating only during the tap changing process.

C. STATIC SWITCHES

As mentioned previously, the static switching in the equipment prototype is done by TRIACs. TRIACs are used instead of other types of static switches due to their low cost and greater simplicity. Since TRIACs are bidirectional semiconductors, they also reduce the number of necessary static switches by half.

The TRIACs used on the prototype are BTA24. The main parameters of these switches are given in Table 4. The switch snubbers resistors and capacitors are not part of the TRIAC and were installed in parallel with each switch.

TABLE 4. Basic parameters of TRIAC BTA24.

Parameter	Value
RMS on-state current	25 A
Repetitive peak off-state voltages	600 V
Non-repetitive peak on-state current at 75° C of case temperature	100 A
Max gate current Q1	50 mA
Max gate current Q4	100 mA
Maximum voltage drop	1.55 V
Snubber resistance	100 Ω
Snubber capacitance	10 µF

D. CONTROL

SVR output voltage is the only variable used by the control to determine which tap to trigger. Figure 6 presents the block diagram for the proposed switching methodology.

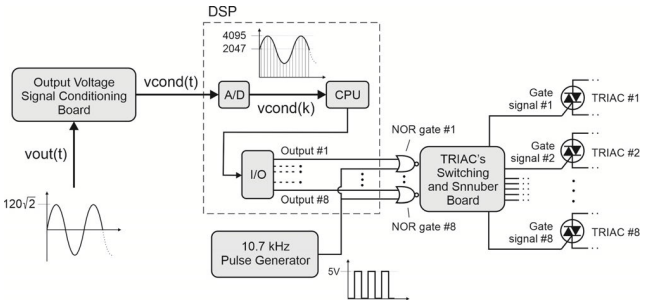

FIGURE 6. Simplified diagram of the developed SVR control.

The output voltage of the SVR, *vout(t),* is conditioned by a signal acquisition and conditioning board in order to be applied to the input of the microprocessor's analog to digital converter (ADC). The microprocessor used in the prototype was the LAUNCHXL-F28379D from Texas Instruments. The conditioned voltage is sampled by an ADC of 12 bits with a sampling rate of 64 samples per cycle of 60 Hz.

Once the signal resulting from the discrete sampling of the voltage is obtained, the microprocessor CPU calculates the RMS voltage on the output of the SVR using windows of one cycle with half-cycle sliding.

Once the voltage value of the SVR is known, the microprocessor sends signals to 8 of its outputs (pins I/O), which will be used to trigger switches S_1 to S_8. The triggering of the TRIACs is performed through a pulse transformer, which is responsible for the galvanic insulation between the control and power circuits. This way, the 8 output signals from the microprocessor, together with a pulse of 10.7 kHz, are applied to 8 logic NOR gates that send these signals to trigger the TRIACs.

The tap to be triggered is calculated in the following way:

$$V_{load} = V_{in} \times (V_{current\_tap} + 1) \tag{5}$$

$$V_{in} = \frac{V_{load}}{(V_{current\_tap} + 1)} \tag{6}$$

$$V_{ref} = V_{in} \times (V_{future\_tap} + 1) \tag{7}$$

Substituting (6) into (7):

$$V_{future\_tap} = \frac{V_{ref} \times (V_{current\_tap} + 1)}{V_{load}} - 1 \tag{8}$$

where V_{load} is the RMS voltage on the load side, V_{in} is the RMS input voltage of the SVR, $V_{current\_tap}$ is the current tap rated voltage, V_{ref} is the reference voltage of the SVR control, and V_{future_tap} is the compensation voltage of the future tap. All variables are in pu.

Notably, the voltage of the taps depends on the input voltage, indicated in (5), since the SVR is based on an auto-transformer. The reference voltage, V_{ref}, set in the prototype control was equal to 1.0 pu.

Another point worthy of attention regarding the previous equations is that the compensation voltage of the future tap, V_{future_tap} presented in (8), is a continuous function. In contrast, the available voltages of the SVR taps are steps (−0.40, −0.25, −0.15, 0.0, 0.15, 0.25, and 0.40 pu). Therefore, it is necessary to define ranges of compensation voltage values for each of the available taps.

Finally, despite the developed SVR being able to switch to tap −3, as shown in Table 2, this tap position was deactivated in the control of the developed equipment. This tap position was deactivated because its compensation voltage is equal to −0.40 pu. As such, by substituting this compensation voltage in (8), with the SVR in tap position 0, we obtain:

$$-0.40 = \frac{1}{V_{load}} - 1 \tag{9}$$

$$V_{load} = 1.667\ pu \tag{10}$$

Through this, it can be concluded that tap −3 will only be triggered in order to compensate voltage swells with magnitudes above 1.667 pu, which are uncommon in electric systems. Additionally, in cases where the SVR triggers the tap −3 and the input voltage returns to its rated value, the load will thus be subjected to a voltage sag of 0.6 pu. Consequently, due to these two situations, tap −3 was deactivated from the control, and all more severe voltage swells were partially compensated by the triggering of tap −2. The ranges of compensation implemented on the SVR control are presented in Table 5. In order to prevent excessive switching of the SVR, the control only changes the tap positions when the output voltage was less than 0.9 pu or higher than 1.1 pu.

IV. COMPUTATIONAL SIMULATION OF THE PROPOSED STATIC VOLTAGE REGULATOR

Before being implemented in a laboratory prototype, the switching methodology proposed in this article, as well as the specification of the components presented in the previous section, was verified through a computer simulation. MATLAB/Simulink was the simulation platform used.

The simplified schematic of the simulated system is shown in Fig. 7. Notably, the gate signals of the TRIACs, the snubbers, and the graphic elements used to visualize the various voltage and current signals in the circuit are not presented for greater clarity in the visualization.

TABLE 5. Tap windings to be triggered according to the required compensation voltage.

Compensation voltage (pu)	Tap
$V_{future\_tap} > 0.40$	+3
$0.40 \geq V_{future\_tap} > 0.15$	+2
$0.15 \geq V_{future\_tap} \geq 0.10$	+1
$0.10 > V_{future\_tap} > -0.10$	0
$-0.10 \geq V_{future\_tap} \geq -0.15$	–1
$V_{future\_tap} < -0.15$	–2

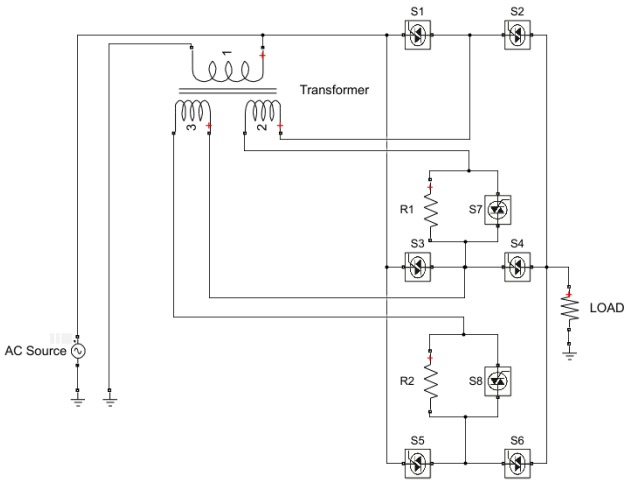

FIGURE 7. Simplified schematic of the simulated system using MATLAB/Simulink.

The parameters of the components in Fig. 7 and the control logic implemented in the simulation are the same that are presented in section III. The RMS voltage values were calculated using a sampling rate of 64 samples per cycle of 60 Hz with a half-cycle sliding window, to simulate the speed of event detection and the accuracy of the measured voltage values that will be implemented in the prototype developed.

It is worth noting that the network's short-circuit level or the impedances of the conductors that connect the various components of the system were not considered in the simulation. That said, as will be observed throughout the document, the short-circuit current values obtained by the computer simulation were more severe than those observed in the laboratory tests. Another point that merits attention is that the selected simulation platform does not contain the TRIAC component in its libraries; thus, the static switches presented in Fig. 7 are composed of two thyristors connected in antiparallel.

To assess the effectiveness of the proposed SVR, two voltage variations were applied on its input terminals: a voltage sag and a voltage swell, both with a duration equal to 15 cycles. The voltage values for each of these two events, along with the tap triggered by the SVR, are shown in Table 6.

These two events will be applied to the laboratory prototype developed. It is noteworthy that the voltage on the input before and after the events was maintained equal to 120 Volts.

TABLE 6. Tap windings to be triggered according to the input voltage – short duration voltage variations.

Event	Input voltage	Duration (cycles)	Triggered tap
-	120 V (1.00 pu)	-	0
I	83 V (0.69 pu)	15	+3
II	149 V (1.24 pu)	15	–2

Finally, the equipment was simulated considering three different load conditions to analyze the performance of the SVR under different load conditions: no-load, supplying a purely resistive load of 300 W, and supplying a distorted load with fundamental active power equal to 156 W.

A. SIMULATION RESULTS OF SVR OPERATING AT NO-LOAD CONDITION

The first simulation considered the SVR at a no-load condition, that is, with no load connected to its output terminals. Fig. 8 illustrates the behavior of the input and output voltages, both in instantaneous values and in RMS values, for the two events presented in Table 6.

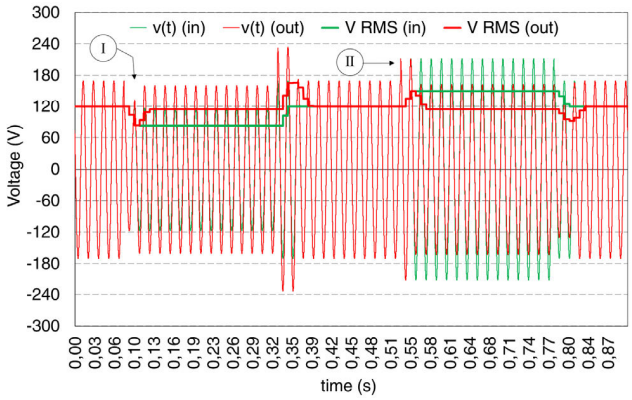

FIGURE 8. Simulated instantaneous and RMS input and output voltages of the SVR, operating under no load, when events I and II of short duration voltage variations occur.

By analyzing the previous figure all tap took around two cycles from the start of the events to be completed. This meets the projected actuation time, which should be up to 4 cycles.

It is observed that the equipment switched its taps to maintain the RMS voltage within the considered adequate range of between 0.9 pu (108 V) and 1.1 pu (132 V).

In what follows, the activation of tap +3 (Fig. 9) and the return from tap +3 to position 0 (Fig. 10) are presented in greater detail.

The load voltage had a significant improvement in the activation of the intermediate tap, which occurred approximately at time instant 0.10 s. The triggering of the final tap, represented by the switching resistors switching off, occurred

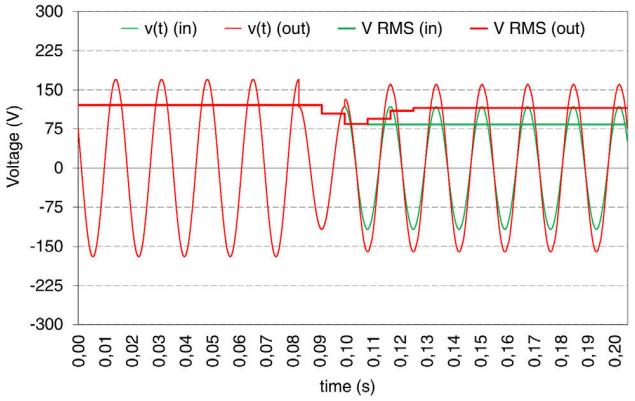

FIGURE 9. Simulated instantaneous and RMS input and output voltage of the SVR, operating under no load, during the change from tap 0 to tap +3.

only 3/4 of a cycle after this moment. Considering the entire tap change process, the switching from position 0 to tap +3 took around two cycles for completion, submitting the load to a two cycles event, and no longer to a 15 cycles sag, which may be critical for the operation of sensitive equipment that may be being connected to the SVR output.

At the instant the SVR input voltage returns to its nominal value, as the equipment has its +3 tap activated, the SVR output voltage will present voltage swell of 1.4 pu magnitude, as shown in Fig. 10.

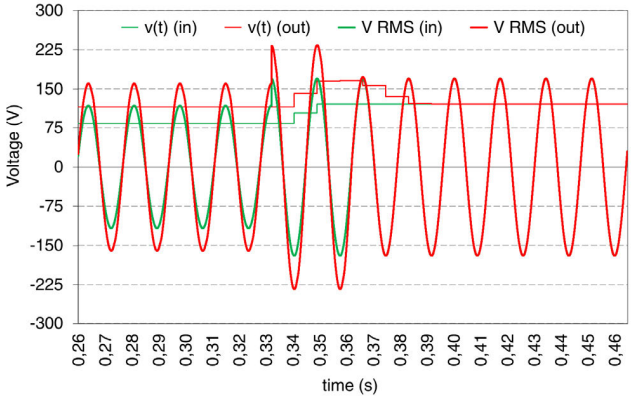

FIGURE 10. Simulated instantaneous and RMS input and output voltages of the SVR, operating under no load, during the return from tap +3 to tap 0.

The analysis of Fig. 10 shows that the 1.4 pu swell was corrected in less than 2 cycles. As mentioned above, this overvoltage with this duration is not supposed to damage the equipment that should be connected to the SVR output.

The inverse situation is also true: if the SVR is correcting a voltage swell that demanded the activation of its tap −2 and its input voltage returns to the nominal value, a sag of 0.75 pu on the output is expected for a period of fewer than 4 cycles. However, equipment malfunctions are not expected either for this magnitude and duration.

In case these two situations violate the operational limits of the load connected to the SVR output, the tap winding transformation ratios can be changed at the cost of a reduction of its voltage regulation range.

B. SIMULATION RESULTS OF SVR SUPPLYING PURELY RESISTIVE LOAD

In the first simulation of the SVR supplying a load, a purely resistive load of 300 W was connected to its output. Also, the same events shown in Table 6 were applied to the regulator's input in this loading situation. The instantaneous and RMS voltages on the input and output of the SVR can be seen in Fig. 11.

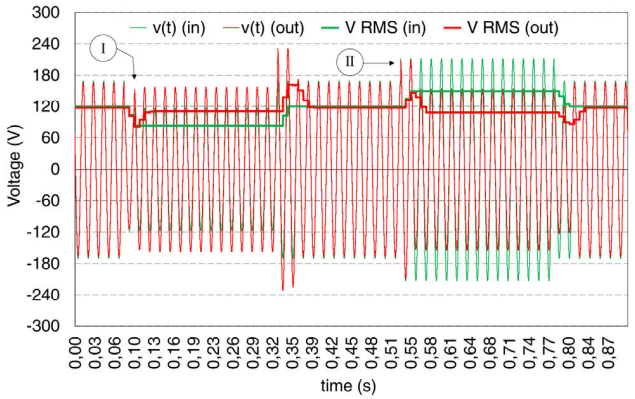

FIGURE 11. Simulated instantaneous and RMS voltages on the input and output of the SVR, supplying resistive load when the short duration voltage variation events I and II occur.

In the same way as seen in the simulations that the SVR was operating at no load, the voltage variations were correct in approximately 2 cycles. As will be shown in greater detail in Fig. 13, there is a small difference between the primary and secondary voltage caused by the drop voltage on the TRIACs, which values approximately 1.5 V per switch.

The instantaneous currents on the input, output and in the two tap windings of the SVR, are shown in Fig. 12.

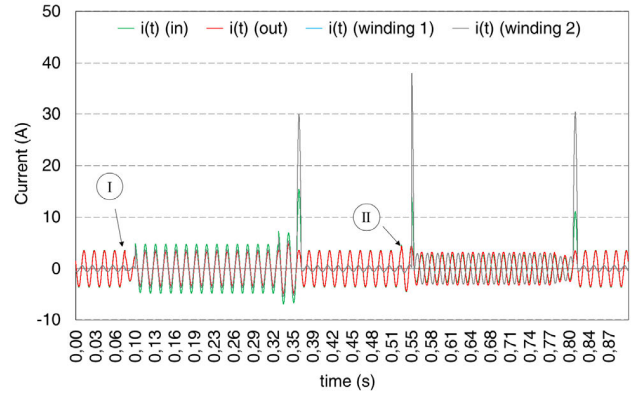

FIGURE 12. Simulated instantaneous currents on the input and output of the SVR, along with tap windings 1 and 2 supplying resistive loads when the short duration voltage variation events I and II occur.

The short-circuits of the tap windings can be observed from the previous figure. As shown earlier, switching resistors have

been specified to limit the windings currents to three times the rated current value (35.4 A RMS or 50.1 A peak) when the input voltage is equal to 1.4 pu.

As the highest simulated and tested input voltage value was equal to 1.24 pu, the highest expected short-circuit current, according to (1) and (3), would be 2.66 pu (31.4 A effective or 44.4 A peak). The analysis of Fig. 12 shows that the current in the tap windings had a peak value of less than 40 A in the worst case. This is attributed to the impedance of the tap windings and the voltage drop on TRIACs S_7 and S_8. Put differently, the specification of switching resistors, in addition to considering an extreme input overvoltage condition, also did not consider the voltage drops on the windings and static switches, therefore being extremely conservative in further increasing the operational safety of autotransformer and static switches.

Furthermore, depending on the instant of the voltage waveform in which the switches are activated, there may be no short-circuit current, as was the case when changing from tap 0 to +3.

The input and output voltages of the SVR at the beginning of event II are illustrated in Fig. 13.

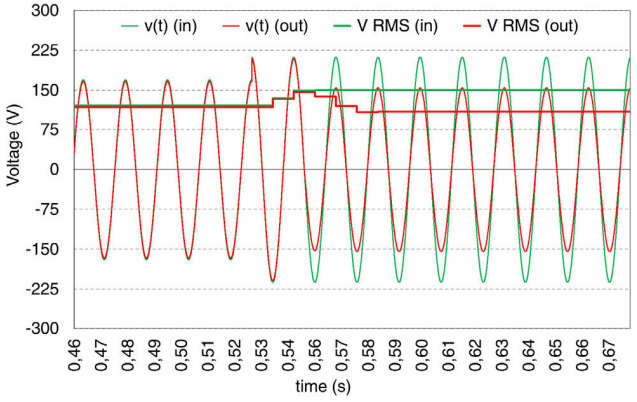

FIGURE 13. Simulated instantaneous and RMS input and output voltages of the SVR, supplying a resistive load during the change from tap 0 to tap −2.

The voltage drop on the TRIACs can be seen in the first moments of Fig. 13, when the SVR is operating at tap 0. As can be observed, there is a slight difference between the input and the load voltage. This voltage difference is equal to 3.1 V (1.55 V per switch).

The input, output and winding 2 currents of the SVR for the same situation, switching from tap 0 to −2, are shown in Fig. 14.

The highest peak current value observed in Fig. 14 is below the maximum projected value for the winding short-circuit current (44 A of peak value for this input voltage).

However, it can be observed that, for this situation, the short-circuit current of winding 2 lasted for only 4 of a cycle. In the worst-case scenario, this short-circuit current is expected to remain for only 1/2 cycle, that is, until the current of the TRIACs that had their gate signal removed

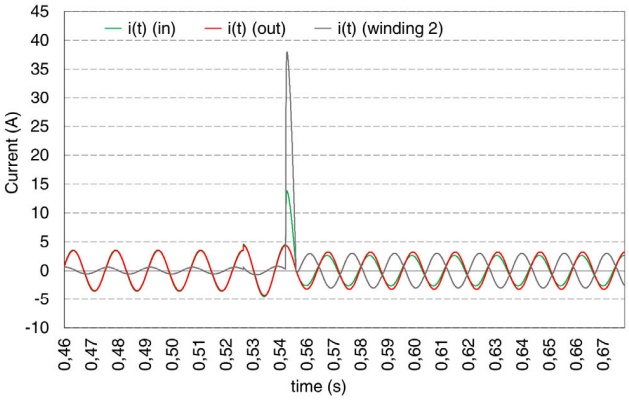

FIGURE 14. Simulated instantaneous currents on the input, output, and in tap winding 2 for the changing of tap 0 to −2 with the regulator supplying a resistive load.

passes through zero; therefore, it is not expected to damage either the autotransformer windings or the static switches due to the brief short-circuit duration of the tap windings.

At the end of event II, when the SVR input voltage returns to its nominal value, the load suffers a voltage sag of 0.72 pu as the tap −2 is activated. This is because the negative compensation of winding 2 (0.25 pu) was increased by 4.65V due to the voltage drop on switches S_3, S_6, and S_8, which are triggered on. However, as can be seen in Fig. 15, this condition lasted for approximately 2 cycles.

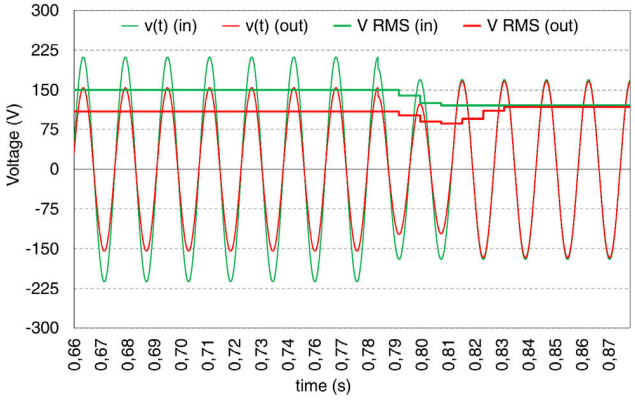

FIGURE 15. Simulated RMS and instantaneous voltages on the input and output of the SVR, supplying a resistive load for the change of tap −2 to tap 0.

Figure 16 presents the input and output currents of the SVR, as well as the current in the tap winding 2, for the return of the SVR from position −2 to tap 0.

The previous figure shows that the short-circuit of the tap winding 2 (30.3 A of peak value) presented a value lower than the projected maximum, again showing that the calculation of the switching resistors was very conservative. Additionally, as described above, this overcurrent will have a maximum duration of 1/2 cycle.

Therefore, it can be concluded that the greatest requirement of switches occurs when the regulator has to correct swells,

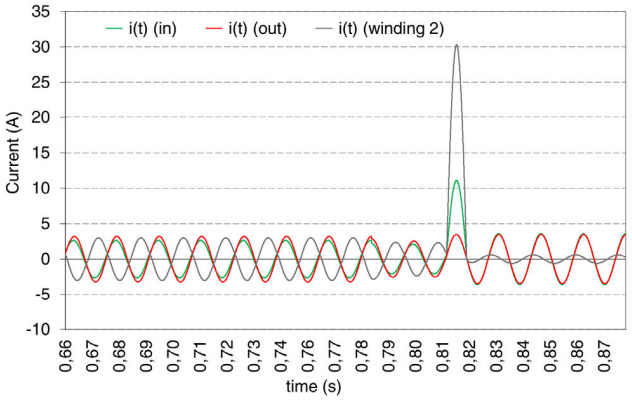

FIGURE 16. Simulated instantaneous input and output currents, along with instantaneous current in tap winding 2, when changing from tap position −2 to position 0 and the SVR supplying resistive load.

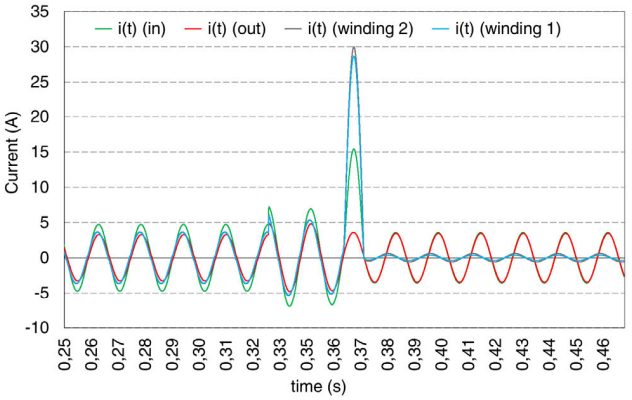

FIGURE 18. Simulated instantaneous input and output currents, along with instantaneous currents in the tap windings, when changing position from tap position +3 to tap 0 and the SVR supplying resistive load.

since the voltage on its magnetization winding rises, increasing the voltage of the secondary coils and, consequently, the value of the short-circuit current in the tap windings.

As shown in the previous subsection, wherein the regulator was operating at no-load condition, when the SVR is correcting a more severe sag, with its +3 tap triggered on, and the input voltage returns to 1 pu, the load will experience a swell of approximately 1.4 pu. This situation is shown in Fig. 17, which presents the input and output voltages of the regulator at the end of event I.

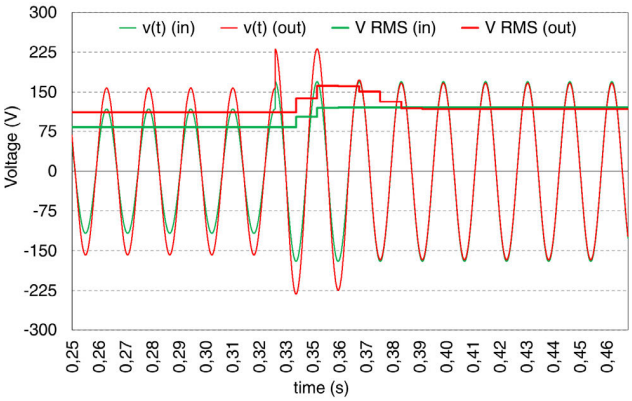

FIGURE 17. Simulated RMS and instantaneous voltages on the input and output of the SVR, supplying resistive load during the change from tap position +3 to tap 0.

The output voltage seen in Fig. 17 is slightly smaller than that seen in Fig. 10 due to voltage drops on switches S_2, S_5, S_7, and S_8, totaling 6.2 V of reduction. From the figure above, as well as from Fig. 18, it can be seen that this tap changing took a little more than 2 cycles to get completed; therefore, such overvoltage should not be harmful to a load being supplied by the SVR.

The input, output, and also currents in the two tap windings of the SVR, for this same situation, are presented in Fig. 18.

The short-circuit currents of the two windings can be seen in Fig. 18. The windings' short-circuit currents were much smaller than the maximum peak value of 44 A, which subjects the switches and the windings to less thermal stress than the projected limit. It is important to point out that the TRIACs used in the prototype have a nominal RMS current equal to 24 A (33.9 A peak value for a purely sinusoidal current).

C. SIMULATION RESULTS OF SVR SUPPLYING A NONLINEAR LOAD

The last simulation of SVR aims to evaluate the behavior of the equipment supplying a non-linear load, with a high level of current distortion. The simulated load was composed of a resistive load of 156 W in parallel with 4 harmonic current sources. The harmonic current values are shown in Table 7.

TABLE 7. Harmonic currents of simulated non-linear load.

Harmonic	RMS current
2	0.650 A
3	0.433 A
4	0.325 A
5	0.260 A

For this situation, the behavior of the input and output voltages of the SVR can be seen in Fig. 19. As observed in the two other load situations, the voltage variations were corrected very quickly, with tap change completion in less than 4 cycles.

The instantaneous currents in the input, output and in the two tap windings of the SVR are shown in Fig. 20. The results observed in the figure below are very similar to those shown in Fig. 12; in none of the 4 tap changes the windings currents were greater than 3 pu.

To provide a more detailed view of the SVR's operation supplying a non-linear load, the figures below present the behaviors of the voltages and currents on the SVR at the start of event II. In particular, Fig. 21 shows the input and output voltages of the equipment in this situation.

Fig. 21 shows that the tap change from position 0 to tap −2 took less than 2 cycles to be completed. Finally, Fig. 22 shows

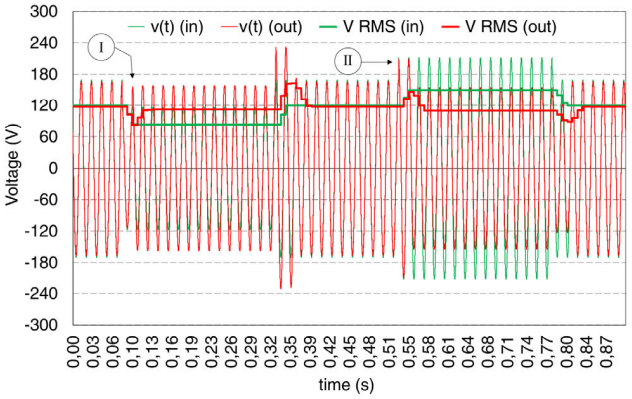

FIGURE 19. Simulated RMS and instantaneous voltages on the input and output of the SVR, supplying a nonlinear load when the short-duration voltage variation events I and II occur.

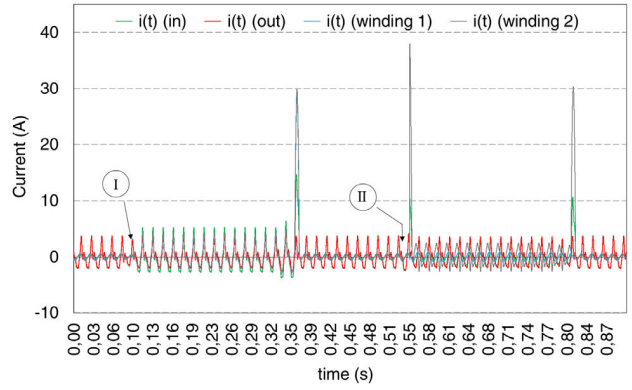

FIGURE 20. Simulated instantaneous currents on the input and output of the SVR, as well as in tap windings 1 and 2, supplying a nonlinear load when the short-duration voltage variation events I and II occur.

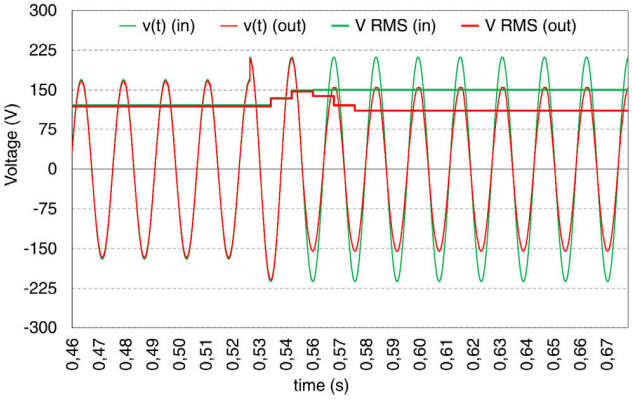

FIGURE 21. Simulated instantaneous and RMS voltages on the input and output of the SVR, supplying a nonlinear load during the change from tap 0 to tap −2.

the behavior of input, output, and tap winding 2 currents for event II.

As explained in section II, the speed of the SVR tap change hinges on some factors such as the instant of the voltage waveform at which the voltage variation occurred and the

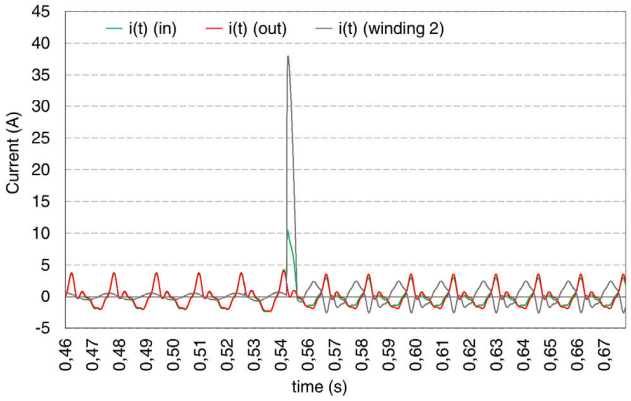

FIGURE 22. Simulated instantaneous input and output currents, along with the instantaneous current in winding 2, when changing from tap position 0 to tap position −2 and the SVR supplying a nonlinear load.

magnitude of the event, since these two factors impact the RMS voltage value calculated every 1/2 cycle and, consequently, the event detection delay. In general, the more severe the event, the greater the chance of the voltage variation being detected by the control in the first RMS voltage calculation window after the beginning of the event.

The SVR is designed to take less than 4 cycles to perform a tap change. Additionally, its bias is to guarantee the safety of the loads that are connected to its output, especially in the situation in which the regulator has tap +3 triggered on and the input voltage returns to its nominal value, subjecting the load to a swell of approximately 1.4 pu. However, as evidenced throughout this section, the static regulator tap changing, in general, took around 2 cycles to be completed, which further increases the operational safety of the loads being regulated by the SVR. In the next section, where the results of the laboratory tests of the developed prototype will be presented, tap changes taking less than 4 cycles will also be observed.

Regarding the short-circuit currents of the SVR's windings, the simulated results were also very promising. Switching resistors were designed to limit the short-circuit currents of the windings to 3 pu in the situation which the input voltage is 1.4 pu. From the standpoint of overvoltage at the fundamental frequency, this condition is extremely rare in a real electrical system. In addition to considering this severe input overvoltage, the switching resistor design did not take into account the system impedances, the autotransformer impedances, or the voltage drop on the TRIACs. Thus, it can be inferred that the design of the switching resistors was extremely conservative, which was confirmed by the simulations.

V. TEST RESULTS OF THE PROPOSED STATIC VOLTAGE REGULATOR PROTOTYPE

The prototype developed employing the components described in section III and the switching methodology presented above is shown in Fig. 23.

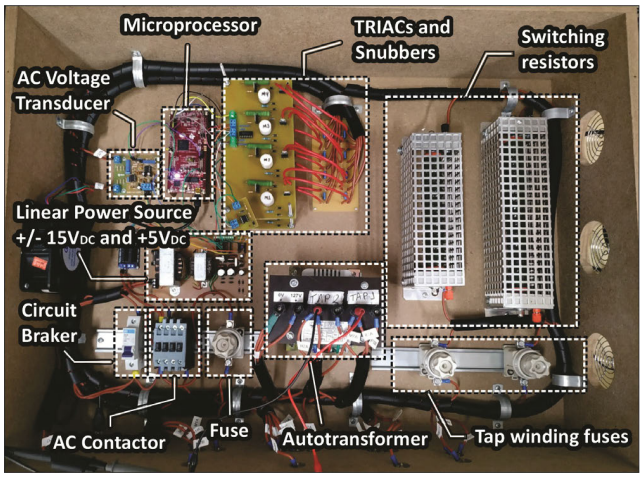

FIGURE 23. Prototype of the developed SVR, contemplating the new switching technology.

The prototype of the voltage regulator developed herein was tested under three different scenarios: (i) operating at no load, (ii) supplying 300 W of incandescent lamps (resistive load), and finally, (iii) supplying a 156 W nonlinear load constituted of a set of electronic lamps of different technologies. In order to perform the tests, the voltage variations at the input of the SVR were synthesized by a programmable power source from California Instruments, model CSW555.

The voltage and current signals, in RMS and instantaneous values, were registered by a G4500 BLACKBOX meter from ELSPEC, with a sampling rate of 1024 samples per cycle at 60 Hz. Figure 24 presents the schematic for the setup used in the performance tests of the prototype equipment.

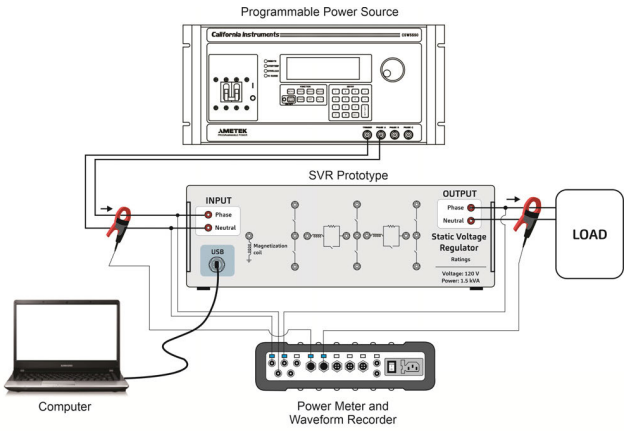

FIGURE 24. Schematic design of the laboratory structure used for realizing performance tests on the static voltage regulator prototype.

The tests performed on the developed SVR had as their objective to evaluate the SVR performance when long and short duration voltage variations were applied to its input. To reach this goal, long duration voltage variations were applied on the SVR input with magnitudes outside of the acceptable range determined by ANSI C84.1 [2], i.e., RMS voltage values higher than 127 V and less than 106 V considering the reference voltage equal to 120 V. Five distinct situations with different RMS input voltage values were tested, which made the SVR switch from tap 0 to all five allowed tap positions, and vice-versa. The input voltage magnitudes, as well as the tap position to be triggered in order to compensate these five voltage variations, are presented in Table 8.

TABLE 8. Tap winding to be triggered according to the input voltage – long duration voltage variations.

Situation	Input voltage	Triggered tap
-	120 V	0
I	104 V	+1
II	95 V	+2
III	83 V	+3
IV	136 V	–1
V	149 V	–2

In addition to the long duration voltage variations tests, the performance of the SVR was evaluated for short duration voltage variations. For each of the three load conditions, two consecutive momentary voltage variations were applied, each with a duration of 15 cycles and amplitudes as indicated in Table 6. The input RMS voltages before and after the event were maintained at 120 V for all cases.

A. SVR OPERATING AT NO-LOAD CONDITION

In the first set of tests, the static voltage regulator had no load connected to its output. Figure 25 presents the variations of the SVR's RMS input and output voltages during the five aforementioned long duration voltage variations applied at the input of the equipment.

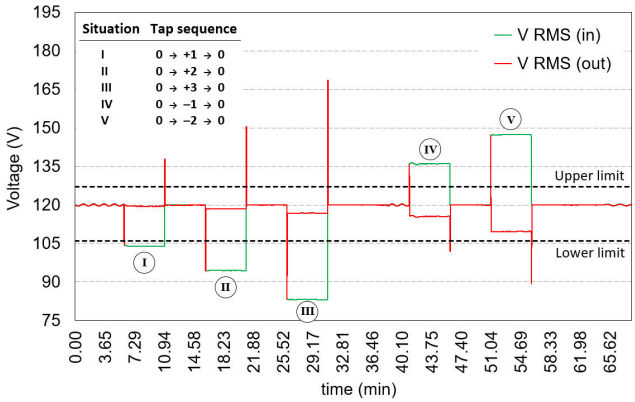

FIGURE 25. Recorded input and output RMS voltage of the SVR operating at no load during the long voltage variations test.

From the analysis of Fig. 25, it is observed that despite the large RMS voltage variations imposed on the input of the SVR, the output RMS voltage (in steady state) remained within the acceptable voltage range, per ANSI C84.1 [2].

As previously explained, spikes of up to 1.4 pu on the RMS output voltage can be verified at the end of the situations I to V. However, these spikes' durations were less than

4 cycles, which do not risk the integrity of loads connected to the output of the equipment.

As an example of this situation, Fig. 26 shows the instantaneous and RMS voltages at the beginning of situation III (Fig. 25) when the regulator switches from tap 0 to tap position +3.

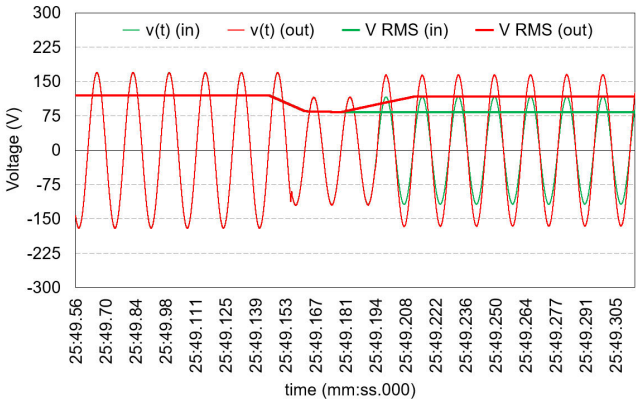

FIGURE 26. Recorded instantaneous and RMS input and output voltage of the SVR, operating under no load, during the change from tap 0 to tap +3.

At the end of situation III, the input voltage returns to its rated value, but the SVR is still in position +3. Then, for a short period of approximately 3 cycles, the load was subjected to a voltage swell. This situation can be seen in Fig. 27, which presents the instantaneous and RMS voltages when the prototype returns from tap position +3 to 0.

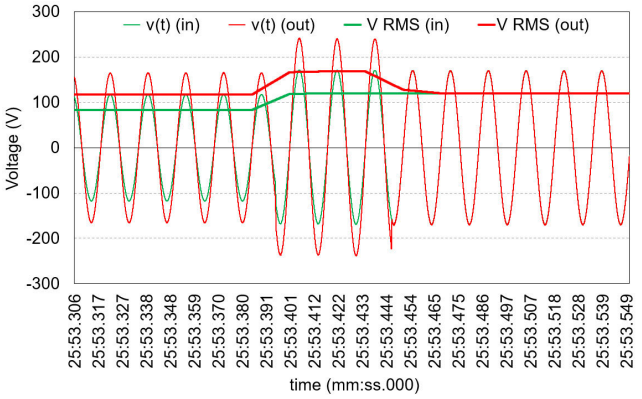

FIGURE 27. Recorded instantaneous and RMS input and output voltages of the SVR, operating under no load, during the return from tap +3 to tap 0.

As the switches were not conducting any current, there was no voltage drop on the TRIACs. However, when operating under load, the activation of tap +3 (switching on TRIACs S_2, S_5, S_7, and S_8) will cause a voltage drop on the conducting switches of approximately 1.5 volts of amplitude per switch, thus causing a small attenuation on the load voltage in relation to the amplitudes shown in Fig. 27. This specific situation will be given greater consideration in the next section.

In the next stage of the static regulator no-load tests, two consecutive short duration voltage variations were applied on the input of the equipment with fixed durations equal to 15 cycles and magnitudes of 0.69 pu and 1.24 pu, respectively, as indicated in Table 6. Figure 28 presents the input and output voltages of the SVR when applying the referred momentary voltage variations, resulting in the triggering of tap +3 for correcting the output voltage during the first event (voltage sag), as well as in the triggering of tap −2 for correcting the output voltage during the second event (voltage swell).

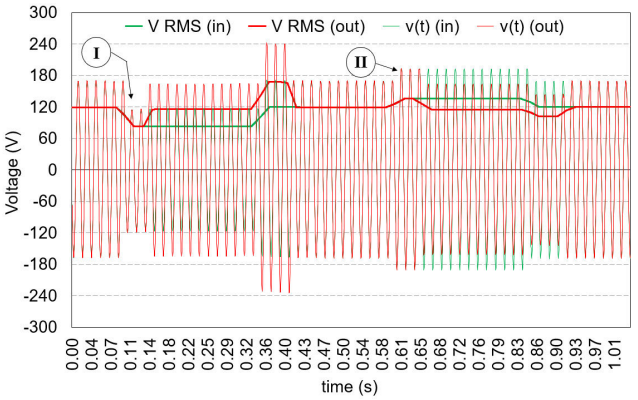

FIGURE 28. Recorded instantaneous and RMS input and output voltages of the SVR, operating under no load, when events I and II of short duration voltage variations occur.

It can be noted from Fig. 28 that the SVR switched its taps to maintain the output voltage close to the reference voltage of 120 V, within the range of 0.9 pu and 1.1 pu in both the voltage sag (situation I) and swell (situation II).

A more precise correction of the output voltage during voltage variation events would be perfectly manageable by considering a higher number of taps on the SVR or by reducing the tap windings rated voltages. Nonetheless, the SVR developed herein manages to attenuate the impacts from these events satisfactorily, be that in terms of amplitude or duration.

Finally, as verified in the tests for the long duration voltage regulation (Fig. 25), when the SVR returns from tap position +3 to position 0, a voltage swell on the output signal reaching 1.40 pu is observed for a time interval not exceeding 4 cycles. In the case of the equipment compensating a voltage swell, with tap −2 activated, when the input voltage returns to 1 pu, the output voltage will be decreased to 0.75 pu while the regulator does not return to tap 0, which may take up to 4 cycles. It is important to emphasize, once more, that such operating conditions do not risk the thermal or dielectric integrity of the loads supplied by the equipment.

B. SVR SUPPLYING PURELY RESISTIVE LOAD

The second set of tests for the SVR prototype evaluated the SVR operating under load conditions. For this purpose, a set of incandescent lamps, totaling 300 W, was connected to the output of the SVR.

The behaviors of the RMS input and output voltages of the SVR during the long duration voltage variations tests are presented in Fig. 29.

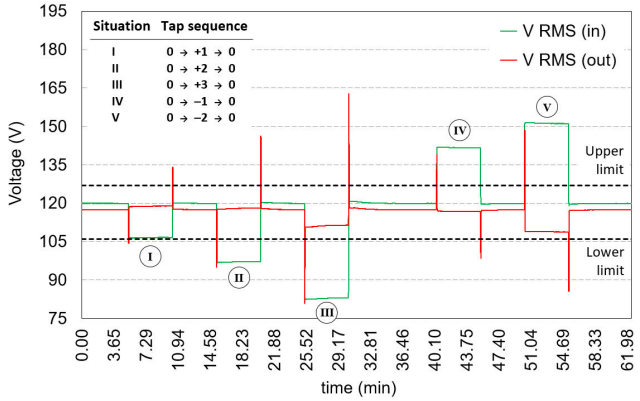

FIGURE 29. Recorded RMS input and output voltages of the SVR, supplying a resistive load during the long voltage variations test.

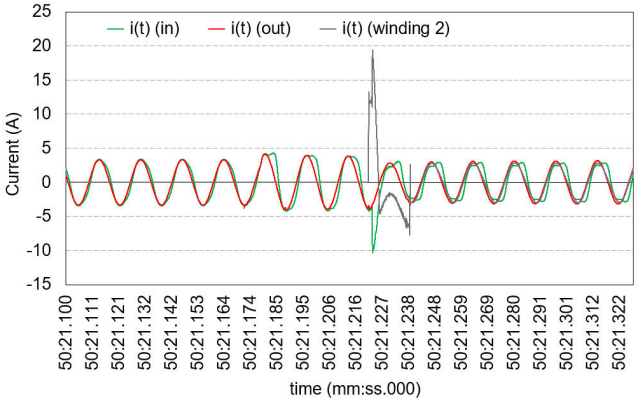

FIGURE 31. Recorded instantaneous currents on the input, output, and in tap winding 2 for the changing of tap 0 to −2 with the regulator supplying a resistive load.

In contrast to the results of the no-load tests, the output voltages in this test present a voltage drop of approximately 1.5 V for each switch on the TRIACs. This situation is clearly seen when the equipment is on tap 0, and the output voltage is slightly lower than the input voltage. Nevertheless, the output voltage remained within the acceptable range throughout the test, as observed in Fig. 29.

Considering Situation V, indicated in Fig. 29, the tap change was once again concluded in less than 4 cycles (approximately 2.5 cycles), as shown in Fig. 30, which presents the switching from the tap position 0 to −2.

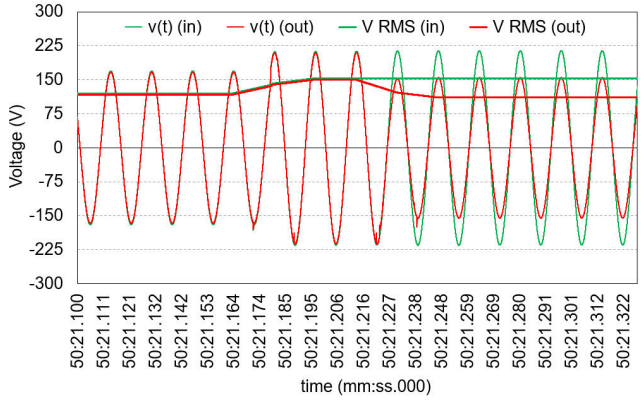

FIGURE 30. Recorded instantaneous and RMS input and output voltages of the SVR, supplying a resistive load during the change from tap 0 to tap −2.

The SVR's input and output currents and current in winding 2 in Situation V of Fig. 29 are presented in Fig. 31.

The moment the intermediate tap switches are triggered, the instantaneous current in winding 2 reaches a peak value of 19.42 A. This value represents 1.63 pu of the rated peak current of this winding, which proves the effectiveness of the switching resistor R_2 as a short-circuit current limiter for winding 2 since this component was projected to limit the winding short-circuit current to a maximum value of 3 pu, as presented in (3). It is important to emphasize that the short-circuit of the windings remains only as long as the currents of the TRIACs that had their gate signal removed do not cross zero. Ideally, this period has a maximum duration of 1/2 a cycle. However, to increase the operational safety of the SVR, the control waits for 3/4 of a cycle to ensure that these switches are off and the short-circuit current is extinguished.

When the input voltage returns to its rated value with the SVR still in tap position −2, the load voltage suffers a sag caused by the compensation voltage of tap −2 (−0.25 pu), which is slightly increased by the voltage drop on switches S_3, S_6, and S_8. Therefore, in agreement with Fig. 32, it is once again noticed that this voltage sag does not last more than 4 cycles.

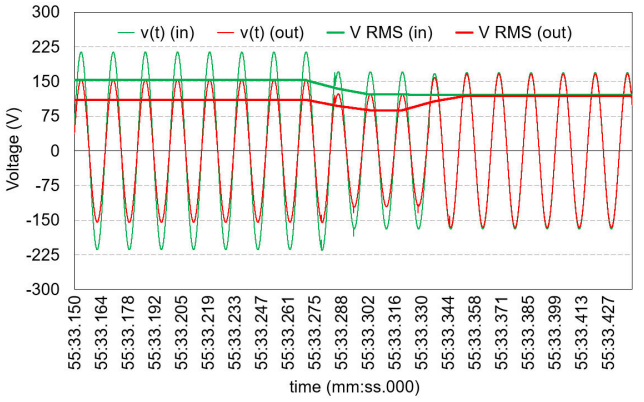

FIGURE 32. Recorded RMS and instantaneous voltages on the input and output of the SVR, supplying a resistive load for the change of tap −2 to tap 0.

The input and output currents of the SVR when returning from tap −2 to tap 0, as the current in winding 2, are presented in Fig. 33.

As shown in Fig. 33, the return from tap −2 to tap 0 also resulted in a short-circuit in winding 2. However, the current amplitude observed (11.44 A) was much less than 3 pu. Once again, the switching resistors proved their effectiveness in limiting the short-circuit in the tap windings.

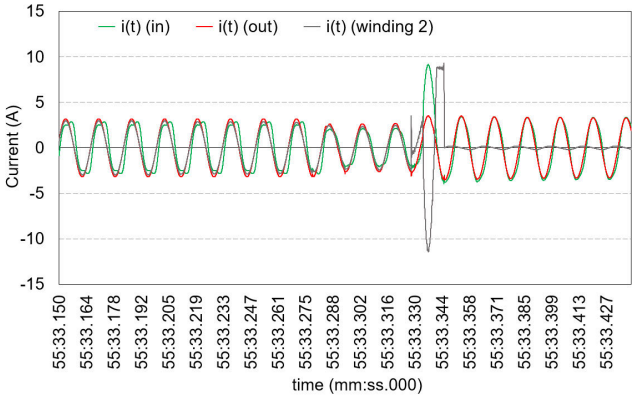

FIGURE 33. Recorded instantaneous input and output currents, along with instantaneous current in tap winding 2, when changing from tap position −2 to position 0 and the SVR supplying resistive load.

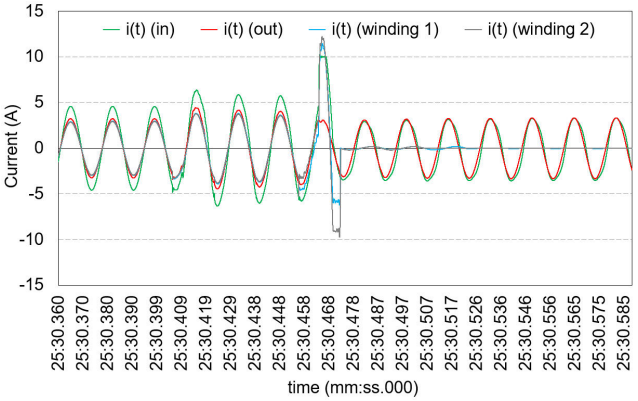

FIGURE 35. Recorded instantaneous input and output currents, along with instantaneous currents in the tap windings, when changing position from tap +3 to position tap 0 and the SVR supplying resistive load.

On the other hand, in the instance when the SVR is at tap position +3 and the input voltage returns to 1.0 pu (end of Situation III of Fig. 29), an increase in the output voltage is observed. As previously mentioned, this does not present any risk to the integrity of the load. In addition, as the SVR is supplying a load, the voltage swell of 1.4 pu is minimized by the voltage drop on the TRIACs, as shown in Fig. 34, which presents the behaviors of input and output voltages of the SVR for this situation. The instantaneous input and output currents, as well as the currents in the two tap windings for this case, are presented in Fig. 35.

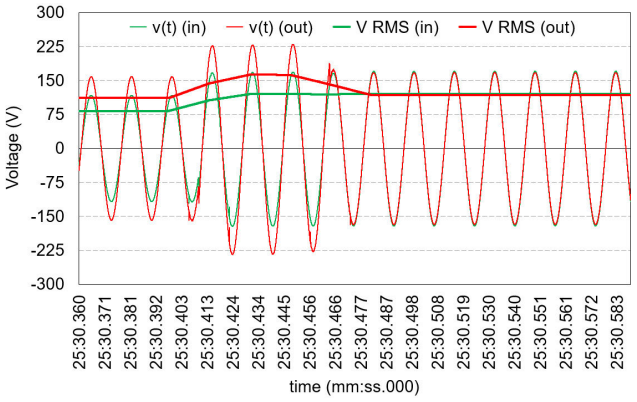

FIGURE 34. Recorded RMS and Instantaneous voltages on the input and output of the SVR, supplying resistive load during the change from tap +3 to tap 0.

As the regulator was on tap +3 when the input voltage returned to 1 pu, the load experienced a voltage swell. In order to correct this situation, the control starts the tap changing process from tap +3 to tap 0. The first stage of this process is activating the intermediate tap +3, switching on resistors R_1 and R_2. When the controller switches on S_3 and S_4 to conclude the switching to tap 0, a short-circuit occurs in tap windings 1 and 2 since both windings are in operation at tap +3, and both have to be disconnected when the SVR is at tap 0. The short-circuit of the windings can be observed in Fig. 35. However, the peak currents registered during this tap change were relatively minor: equal to 11.45 A (0.96 pu) and 12.13 A (1.02 pu) in windings 1 and 2, respectively, thus proving the functionality of the switching resistors in limiting the short-circuit currents in the windings during tap changing.

While still considering the operation of the SVR supplying a 300 W resistive load, tests were performed to verify the effectiveness of the static voltage regulator in attenuating short duration voltage variations. As such, two momentary voltage events were applied to the SVR input, as shown in Table 6. In order to illustrate the results obtained under these conditions, Fig. 36 presents the input and output voltages of the SVR at the moment these two voltage events are imposed, thus resulting in the activation of taps +3 and −2, respectively.

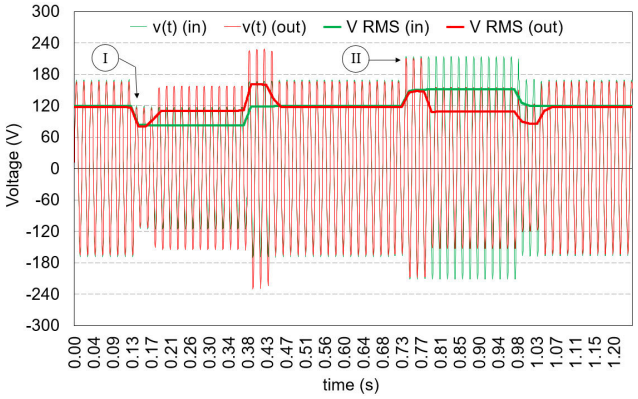

FIGURE 36. Recorded instantaneous and RMS voltages on the input and output of the SVR, supplying resistive load when the short duration voltage variation events I and II occur.

For the same test, the instantaneous input and output currents of the SVR, along with the instantaneous currents in both tap windings, are shown in Fig. 37.

The highest peak current values observed in Fig. 37 occur when the SVR returns to tap 0: 11.41 A (0.96 pu) for the return from tap +3 and 14.93 A (1.25 pu) when the equipment

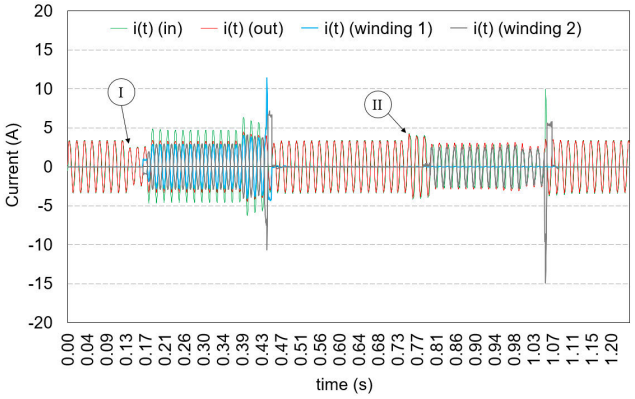

FIGURE 37. Recorded instantaneous currents on the input and output of the SVR, along with tap windings 1 and 2 supplying resistive loads when the short duration voltage variation events I and II occur.

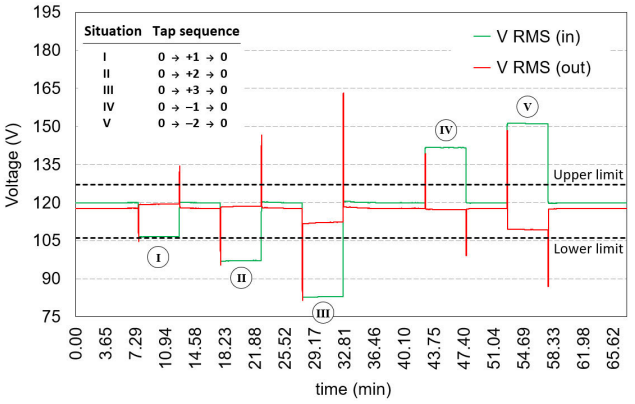

FIGURE 38. Recorded RMS voltages on the input and output of the SVR, supplying a nonlinear load.

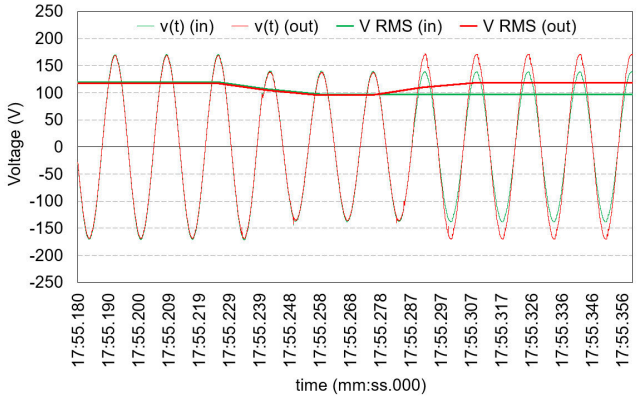

FIGURE 39. Recorded instantaneous and RMS voltages on the input and output of the SVR, supplying a nonlinear load during the change from tap 0 to tap +2.

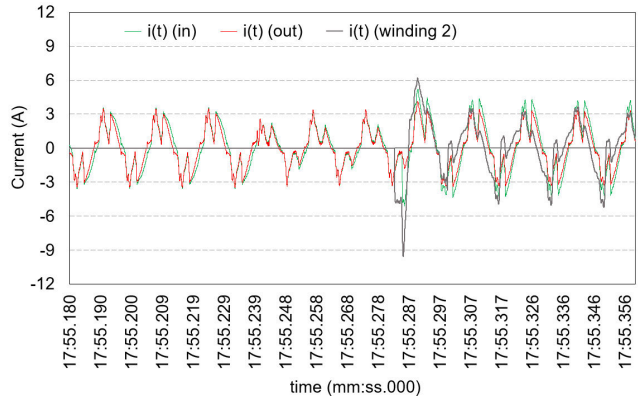

FIGURE 40. Recorded instantaneous input and output currents, along with the instantaneous current in winding 2, when changing from tap position 0 to tap position +2 and the SVR supplying a nonlinear load.

returned from tap −2. Once again, it can be observed that the switching resistors were capable of limiting the short-circuit current.

C. SVR SUPPLYING A NONLINEAR LOAD

The final set of SVR performance tests considers the equipment supplying a 156 W nonlinear load, constituted of electronic lamps of different technologies. The RMS voltages registered on the input and output of the SVR during the long duration voltage variations, shown in Table 8, are presented in Fig. 38.

For illustration purposes, Fig. 39 presents the instantaneous and RMS voltages during the switching process from tap 0 to tap position +2, indicated as Situation II in Fig. 38.

From the analysis of Fig. 39, it can be noticed that the process of tap changing was concluded 3 cycles after the beginning of the voltage sag. Still considering Situation II of Fig. 38, the instantaneous input and output currents of the SVR, along with the instantaneous current registered in winding 2, are presented in Fig. 40.

Similar to the previous tests, the analysis of Fig. 40 shows that the triggering of the intermediary tap caused a short-circuit on winding 2. However, the peak value of the instantaneous current in winding 2 was only 9.56 A (0.80 pu).

Finally, to conclude this third set of performance tests on the SVR, the equipment was subjected to the two short duration voltage variation events indicated in Table 6. The input and output voltages of the SVR along this test are presented in Fig. 41.

The instantaneous currents on the SVR's input and output, along with the currents in windings 1 and 2, are presented in Fig. 42.

Once again, the current values registered in the windings during switching were satisfactory, thus guaranteeing the safe operation of the static switches and of the autotransformer. The peak value registered for the instantaneous current in the tap windings was 19.22 A (1.57 pu) in winding 2.

It is important to emphasize that the short-circuit currents observed in the laboratory tests presented values much lower than the simulated ones, shown in section IV. This difference is due to the impedances inherent to the physical assembly of the equipment, such as the cables connecting the various components of the SVR, for example, as can be seen in Fig. 23, which result in an increase in the short-circuit

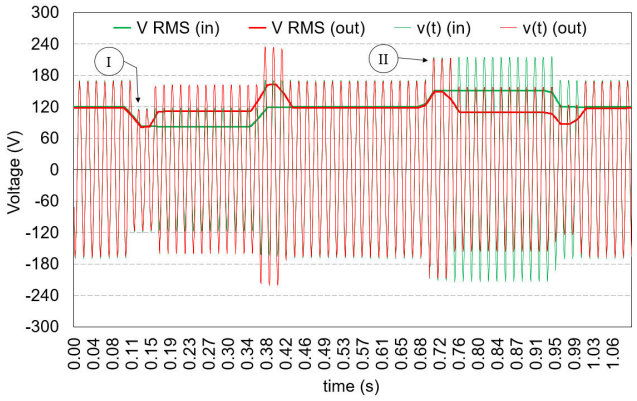

FIGURE 41. Recorded RMS and instantaneous voltages on the input and output of the SVR, supplying a nonlinear load when the short-duration voltage variation events I and II occur.

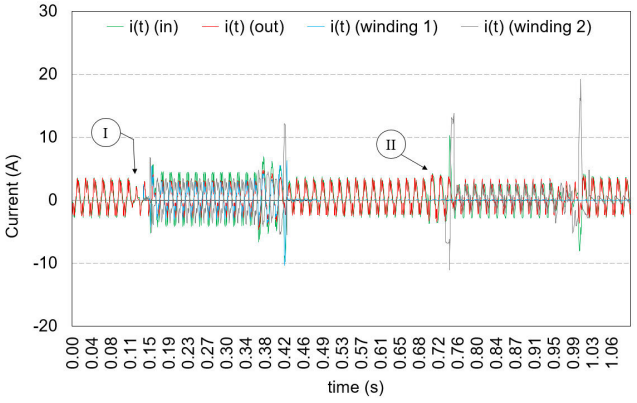

FIGURE 42. Recorded instantaneous currents on the input and output of the SVR, as well as in tap windings 1 and 2, supplying a nonlinear load when the short-duration voltage variation events I and II occur.

impedances of the windings, decreasing their short-circuit currents and ensuring safer operation for the autotransformer and switches.

In regards to the input and output voltages of the SVR, when the two short duration voltage variation events occurred (considering three different load conditions: no-load, resistive load, and nonlinear load), the equipment presented an outstanding performance in all observed situations. In all these conditions, the SVR was able to reduce voltage variations quickly, regulate the load voltage safely in less than 4 cycles, and control the current during tap change, ensuring that neither the switches nor the autotransformer were damaged.

Additionally, it is essential to emphasize that the control developed and presented in this paper does not use the current in static switches or the autotransformer windings to perform the tap changing. This reduces the complexity of the control, and the required number of sensors and signal conditioning circuits.

Another important consideration is that, as the SVR takes up to 4 cycles to perform a tap change, the regulator will not compensate events with durations of fewer than 4 cycles.

Finally, it is imperative to mention that the switching methodology presented in this paper does not require current sensors on the switches and on the autotransformer windings to perform tap changes. Nevertheless, for equipment to be installed in real grids, which are susceptible to transient overvoltages (caused by atmospheric discharges, for example) and overcurrents (caused by short-circuits or transformers' inrush currents passing through the SVR, for example), it is necessary to employ protection devices for both overvoltages and overcurrents. With regard to overcurrent protection, it may be necessary to utilize current sensors at the input of the SVR in order to protect the equipment against currents with dangerous magnitudes. However, the current measured by these sensors would not be used by the control to perform a tap change, but rather by the protection devices to prevent damage to the SVR.

VI. CONCLUSION

This paper presents a new switching methodology for static voltage regulators on low voltage grids. As it does not depend on the current signal measurement of the switches and tap windings, the new switching methodology does not present the operational limitations of other methodologies found in the literature, which can present operational restrictions on electric networks with low loading rates and high levels of harmonic current distortions. The new switching methodology was computationally simulated and implemented onto a static voltage regulator prototype, and its performance was tested under three distinct load conditions: no-load, resistive load, and nonlinear load. The results showed that the proposed methodology is promising. It corrects voltage variations in less than 4 cycles of the fundamental frequency, thus presenting aptness for attenuating long and short duration voltage variations with duration higher than 4 cycles. Based on the obtained performance, the presented methodology can be used in many different applications, whether to comply with steady state voltage regulations, to attenuate short duration voltage variations when dealing with sensitive loads, or even to interface distributed generation systems with the low voltage distribution network. Finally, the development of a three-phase control and prototype, as well as the implementation of SVR's protection devices against overcurrents and overvoltages will addressed in the continuity of the research and will be discussed in future works.

REFERENCES

[1] S. Vavilapalli, U. Subramaniam, S. Padmanaban, and V. K. Ramachandaramurthy, "Design and real-time simulation of an AC voltage regulator based battery charger for large-scale PV-grid energy storage systems," *IEEE Access*, vol. 5, pp. 25158–25170, 2017, doi: 10.1109/ACCESS.2017.2768438.

[2] *American National Standard for Electric Power Systems and Equipment—Voltage Ratings (60 Hz)*, document ANSI C84.1-2020, 2020.

[3] *IEEE Recommended Practice for Monitoring Electric Power Quality*, Standard 1159, 2019.

[4] R. Thompson, "Regulator apparatus including static switching circuit having mid-tapped inductor," U.S. Patent 3 530 369, Sep. 22, 1970.

[5] C. Schoendube, "Electrical apparatus with thyristor circuit," U.S. Patent 3 732 486, May 8, 1973.

[6] G. H. Cooke and K. T. Williams, "Thyristor assisted on-load tap changers for transformers," in *Proc. 4th Int. Conf. Power Electron. Variable-Speed Drives*, London, U.K., 1990, pp. 127–131.

[7] G. H. Cooke and K. T. Williams, "New thyristor assisted diverter switch for on load transformer tap changers," *IEE Proc. B, Electr. Power Appl.*, vol. 139, no. 6, pp. 507–511, Nov. 1992, doi: 10.1049/ip-b.1992.0062.

[8] N. Chen and L. E. Jonsson, "A new hybrid power electronics on-load tap changer for power transformer," in *Proc. IEEE Appl. Power Electron. Conf. Expo. (APEC)*, Charlotte, NC, USA, Mar. 2015, pp. 1030–1037, doi: 10.1109/APEC.2015.7104475.

[9] J. H. Shuttleworth, R. AlZahawi, and X. Tian, "Fast response GTO assisted novel tap changer," *IEEE Trans. Power Del.*, vol. 16, no. 1, pp. 111–115, Jan. 2001, doi: 10.1109/61.905608.

[10] Y. Wang, T. Zhao, M. Rashidi, J. Schaar, and A. Trujillo, "An arcless step voltage regulator based on series-connected converter for branch current suppression," *IEEE J. Emerg. Sel. Topics Power Electron.*, vol. 9, no. 5, pp. 5272–5281, Oct. 2021.

[11] Y. H. Chung, G. H. Kwon, T. B. Park, and K. Y. Lim, "Dynamic voltage regulator with solid state switched tap changer," in *Proc. CIGRE/IEEE PES Int. Symp. Qual. Secur. Electr. Power Del. Systems*, Montreal, QC, Canada, Oct. 2003, pp. 105–108, doi: 10.1109/QSEPDS.2003.159804.

[12] F. Q. Yousef-Zai and D. O'Kelly, "Solid-state on-load transformer tap changer," *IEE Proc.-Electr. Power Appl.*, vol. 143, no. 6, pp. 481–491, Nov. 1996.

[13] K. Abbaszadeh, M. Ardebili, and A. R. Alaei, "Design and built of on–load fully electronic tap-changer with triac switch: Simulation and practical results," in *Proc. 1st Power Electron. Drive Syst. Technol. Conf. (PEDSTC)*, Tehran, Iran, 2010, pp. 340–344, doi: 10.1109/PEDSTC.2010.5471794.

[14] J. de Oliveira Quevedo, F. E. Cazakevicius, R. C. Beltrame, T. B. Marchesan, L. Michels, C. Rech, and L. Schuch, "Analysis and design of an electronic on-load tap changer distribution transformer for automatic voltage regulation," *IEEE Trans. Ind. Electron.*, vol. 64, no. 1, pp. 883–894, Jan. 2017.

[15] J. Faiz and B. Siahkolah, "Practical implementation and experimental results," in *Electronic Tap-Changer for Distribution Transformers*, vol. 2, Berlin, Germany: Springer, 2011, pp. 129–169.

[16] A. A. A. Ismail, H. Alsuwaidi, and A. Elnady, "Automatic voltage stabilization using IGBT based on load tap changer with fault consideration," *IEEE Access*, vol. 9, pp. 72769–72780, 2021, doi: 10.1109/ACCESS.2021.3079507.

[17] P. Bauer and R. Schoevaars, "Bidirectional switch for a solid state tap changer," in *Proc. IEEE 34th Annu. Conf. Power Electron. Spec.*, Acapulco, Mexico, Jun. 2003, pp. 466–471, doi: 10.1109/PESC.2003.1218336.

[18] I. N. Gondim, C. E. Tavares, J. A. F. Barbosa, J. C. Oliveira, and A. C. Delaiba, "Electronic equipment dielectric and thermal withstand capability curves for refunding analysis purposes," in *Proc. 11th Int. Conf. Elect. Power Qual. Utilisation*, Lisbon, Portugal, 2011, pp. 1–6, doi: 10.1109/EPQU.2011.6128812.

[19] P. H. O. Rezende, "Contributions to computational studies of reimbursement for electrical damages: Tolerance limits and electromagnetic inductions," Ph.D. dissertation, Fac. Electr. Eng., Federal Univ. Uberlandia, Uberlândia, Brazil, Dec. 2016, doi: 10.14393/ufu.te.2017.34.

RODRIGO NOBIS DA COSTA LIMA was born in Jataí, Brazil. He received the bachelor's and master's degrees in electrical engineering from the Federal University of Uberlândia, in 2014 and 2017, respectively, where he is currently pursuing the Ph.D. degree. From 2016 to 2017, he held the position of an Energy Quality Engineer at the Energisa Sul-Sudeste Electric Utility, holding the technical responsibility for the sectors of quality of the product and reimbursement of electrical damage. He has been a Researcher with the Laboratory of Electric Distribution Systems, where research is conducted into voltage regulation, harmonic distortions, and distribution generation, besides performing measurements and audits related to the quality of electric energy.

JOSÉ RUBENS MACEDO, JR. (Senior Member, IEEE) received the B.Sc. and M.Sc. degrees in electrical engineering from the Federal University of Uberlândia, Brazil, in 1997 and 2002, respectively, and the D.Sc. degree from the Federal University of Espírito Santo, Brazil, in 2009. In 2015, he completed a short term postdoctoral fellowship at Worcester Polytechnic Institute (WPI), under the supervision of Prof. Alexander Emanuel. His work experience includes different electrical utilities as a Power Quality Manager. Since 2010, he has been with the Faculty of Electrical Engineering, Federal University of Uberlândia, where he works with a research group involved in distribution systems and power quality issues. From 2011 to 2013, he was the President of the Brazilian Power Quality Society.